Effects of the properties of SO$_4$/ZrO$_2$ solid catalysts on the products of transformation and reaction mechanism of R-(+)-limonene diepoxides

O.V. Salomatina [a],[*], T.G. Kuznetsova [b], D.V. Korchagina [a], E.A. Paukshtis [b], E.M. Moroz [b], K.P. Volcho [a], V.A. Barkhash [a], N.F. Salakhutdinov [a]

[a] *N.N. Vorozhtsov Novosibirsk Institute of Organic Chemistry, Siberian Branch of the Russian Academy of Sciences, Acad. Lavrentiev Ave. 9, Novosibirsk 630090, Russia*
[b] *G.K. Boreskov Institute of Catalysis, Acad. Lavrentiev Ave. 5, Novosibirsk 630090, Russia*

Abstract

Transformations of limonene diepoxides on solid SO$_4$/ZrO$_2$ catalysts in dried methylene chloride at room temperature were investigated by varying the amounts of supported sulfate ions and zirconia polymorphs. A method for estimating acid centers from DRIFTS spectra of adsorbed pyridine on the solid catalyst in a dried methylene chloride solution has been developed. It is shown that the mechanism of diepoxide transformations is changed by varying the type and amount of acid centers. At a 0.9–3% level of sulfation, Lewis centers are mainly responsible for the initial cleavage of the 8,9-epoxy group of limonene diepoxides (route B). At higher contents of sulfate ions (up to 30 wt.% SO$_4$), the key transformations proceed with cleavage of the 1,2-epoxy group (route A) and involve the Brønsted centers. The type of support affects the structural features of the sulfate ions, which govern the rearrangement of limonene diepoxides by route A or B. Transformation of limonene diepoxides on the Lewis centers formed on sulfated alumina follows mainly route A. The type of acid centers also affects the stereochemical composition of the product mixture.
© 2007 Elsevier B.V. All rights reserved.

Keywords: Limonene diepoxides; Sulfated zirconium oxide; Rearrangements; Mechanism; Acid catalysis; Alumina

1. Introduction

The epoxy ring readily formed by oxidation of double bonds exhibits high reactivity in acidic and basic media [1]; this is part of many biologically active compounds, both natural and synthetic, and an important building block in organic synthesis [2]. Because of their unique structure and biological activity, epoxy terpenes are very important substrates for chemical synthesis; these are inexpensive and readily available compounds. Reactions with these compounds used as substrates afford products from various classes of organic compounds. Using zeolites, clays, and other solid acids as catalysts of acid transformations of terpenes and their epoxy derivatives not only improves the ecological characteristics of processes and lowers the barriers to activation of known transformations, but also occasionally changes the reaction route compared to routes in homogeneous media [3].

As is known, dissolution of limonene diepoxides **1a,b** in homogeneous acid media leads to reactions necessarily involving an external nucleophile. The cation center initially formed during cleavage of the protonated epoxy ring either reacts immediately with the external nucleophile, giving the products of independent cleavage of epoxy rings **2a,b–3a,b** [4,5] or undergoes intramolecular cyclization, forming the 6-oxabicyclo[3.2.1]octane cation trapped by the external nucleophile to give compounds **4a,b–5a,b** [5] (Scheme 1). Thus dissolving diepoxides **1a,b** in 1N HCl in ether leads to cleavage of the 1,2-epoxy ring, forming hydrochloride **2a,b**. In the acetone–water–sulfuric acid system, the 1,2-epoxy ring is converted into diol, and the 8,9-epoxy group reacts with the acetone molecule to form 1,3-dioxolane ring **3a,b**. Transformations of limonene diepoxides **1a,b** in formic and trifluoroacetic acids

* Corresponding author. Tel.: +7 3833308870; fax: +7 3833309752.
E-mail address: ana@nioch.nsc.ru (O.V. Salomatina).
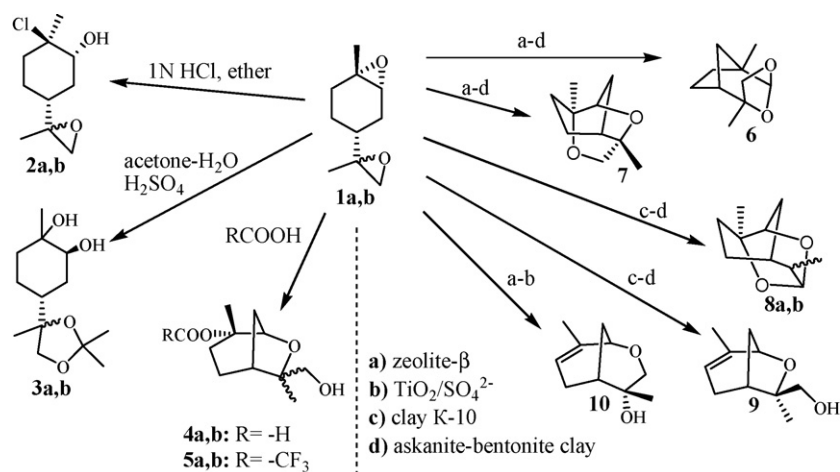
Scheme 1.

lead to 6-oxabicyclo[3.2.1]octane derivatives **4a,b**–**5a,b**. Isomerization on solid acid catalysts (zeolite-β, askanite-bentonite clay, clay K-10, and SO_4/TiO_2) does not involve an external nucleophile and leads to a wide spectrum of optically active bis- and tricyclic oxygen-containing compounds (Scheme 1) [6]. The qualitative and quantitative compositions of the reaction mixture depend on the type of the solid catalyst used. On clays, compound **7** was the major product, while **6**, **8a,b**, and **9** formed in smaller amounts (ratio of **6**, **7**, **8a,b**, and **9** was ∼4:7:2:3, respectively, GLC data). On zeolite and sulfated titania, the reaction gave **6**, **7**, and **10** (product ratio was ∼2:2:5 and ∼3:1:2, respectively, GLC), the major product being either compound **10** or compound **6** (GLC).

It is important that contrary to homogeneous media, solid acid catalysts promote biomimetic mechanisms of the transformations of limonene diepoxides. For example, isobottrospicatol **9** was previously obtained by the action of *Streptomyces bottropensis* on carveol [7], compound **10** was isolated from the aerial parts of *Haplopappus multifolius* [8], and tricyclic diethers **8a,b** possess the framework of paeonimetaboline [9].

The significant effect of the nature of the solid acid catalyst on the composition of the product mixture and product ratio in transformations of limonene diepoxides **1a,b** prompted us to investigate the catalyst structure effects on the reaction route to gain more profound understanding of the processes and to study possible effects of some characteristics of the solid catalyst on the composition of the reaction mixture.

Sulfated zirconia showed remarkable activity in reactions not catalyzed by conventional solid catalysts, e.g., in skeletal isomerizations of alkanes, alkane alkylations with alkenes, low-temperature crackings of polyolefins, Friedel–Crafts type alkylations, citronellal cyclizations, and benzoic acid etherifications [10–19]. The high catalytic activity of sulfated zirconia was attributed to superacidity of this compound. However, some authors claimed that sulfated zirconia has no superacidity or that catalytic activity is not related to superacidity [20–23]. The state of the surface of zirconia polymorphs may influence the nature of the adsorbed sulfate, leading to ionic or covalent sulfates [24–28]. The covalent character of the sulfate depends on the degree of surface dehydration and on the type of coordina-

tion of the oxygen atom(s) to the Zr centers (reducing the S=O bond order) [24–25]. Yamaguchi [26] assumed that the sulfate chelates one Zr atom with a double oxygen bond, attracting electrons and making it a strong Lewis acid. Clearfield et al. [27] suggested that sulfur bridges two zirconium atoms and that by water sorption Lewis acid sites are converted to Brønsted acid sites. In an HRTEM study, Benaissa et al. [28] observed two- or threefold coordination of sulfate groups to zirconia crystallites. Interpretation of the acidic properties of sulfated zirconia is further complicated by the dependence of the nature of this material on the preparation methods and conditions [29–32]. The sulfate ions, adding during the synthetic procedure, stabilize tetragonal zirconia, but increase the particle size of the phase [14].

The role of different types of acidic center and polymorphous modifications of zirconia in the reactions is also the source of controversy. The higher activity of pseudocubic sulfated zirconia in *n*-butane isomerization compared with tetragonal and especially monoclinic modifications cannot be attributed to changes in surface functionalities, but is believed to be the consequence of better stabilization of the high-symmetry crystalline form (due to the more favorable distribution of sulfates in regular and defective parts of crystals) [12]. Both Lewis and Brønsted active acid centers were claimed to be important for the reaction. For nanosized zirconia applied to alumina-silicate layers of montmorillonite (Zr pillared clay) and consisting predominantly of single Zr_4 tetramers, sulfation at low loading starts with formation of isolated sulfate bound with Zr^{4+} cations [13]. The increased acidity (Brønsted centers) is associated with polymerized sulfate species formed at high loading and guaranteeing higher activity in *n*-hexane isomerization and isopropanol dehydration. The Brønsted centers generated by loading excess sulfate are active in skeletal isomerization, while the Lewis centers of submonolayer sulfate, covering the surface, catalyze Friedel–Crafts type alkylation of benzene with benzyl chloride in the liquid phase [11]. The presence of both Lewis and Brønsted sites is essential to cyclization of citronellal to isopulegol [18].

This controversy in determining active reaction centers may be associated not only with the complexity of reaction mechanisms or the effects of the synthetic procedure of catalysts, but also with methods for evaluating the acid centers of the cata-

Table 1
Chemical composition, specific surface area (SSA), and number of acidic centers for sulfated catalysts (wt.% SO$_4$)

Sample number	Chemical composition	SSA (m^2/g)	Number of acidic centers (a.u.)	
			Lewis type	Brønsted type
Sample 1	0.9% SO$_4$/90% M + 10% T-ZrO$_2$	63	n.d.[a]	n.d.
Sample 2	0.9% SO$_4$/C-ZrO$_2$	60	n.d.	n.d.
Sample 3	0.9% SO$_4$/60% T + 40% M-ZrO$_2$	145	1.6	0
Sample 4	1.8% SO$_4$/60% T + 40% M-ZrO$_2$	140	n.d.	n.d.
Sample 5	3.0% SO$_4$/60% T + 40% M-ZrO$_2$	130	0.7	2.8
Sample 6	9.0% SO$_4$/60% T + 40% M-ZrO$_2$	110	n.d.	n.d.
Sample 7	15.2% SO$_4$/60% T + 40% M-ZrO$_2$	100	0	4.5
Sample 8	30.3% SO$_4$/60% T + 40% M-ZrO$_2$	81	n.d.	n.d.
Sample 9	3.0% SO$_4$/γ-Al$_2$O$_3$	189	3.7	0
Sample 10	0.9% SO$_4$/Zr PL	240	0	2.0

[a] n.d.: not determined.

lysts. According to quantum chemical data, the strength of acid centers in sulfated zirconium dioxide is close to that in sulfuric acid, but weaker than that in zeolites [33,34]. The data of the tracer method confirm that the strength of the acid centers of sulfated zirconium dioxide approaches the strength of these centers in 100% sulfuric acid [35]. However, varying the color of the Hammett indicator may affect the chemical nature and the environment of the solid surface, resulting in detection of properties that are far from the working state of the catalyst. Moreover, it is generally difficult to derive exact quantitative data from the color of the indicator. To determine the acidic properties of sulfated zirconium dioxide one can also employ gas-phase adsorption of ammonia and pyridine [11–13,18]. However, thermally programmed desorption of ammonia resulted in peaks observed at high temperatures well above the reaction temperatures. Ammonia adsorbed on a pure support may be removed by preliminary treatment of the surface with steam, significantly reducing the temperature of the desorption peak [11]. In the case of pyridine, the surface centers may be detected from the characteristic IR bands of various adsorbed complexes. In the region of adsorbed complexes, however, IR spectra depend significantly on the desorption temperature. Preliminary sample training in vacuum before adsorption is a substantial disadvantage common to all of these methods because it can drastically change the composition of the surface.

In this work we have studied for the first time the transformations of limonene diepoxides in the presence of methylene chloride on ZrO$_2$ solid catalysts at room temperature while varying the structure of zirconia and activating the surface with supported sulfate ions. The following modifications of highly disperse bulk zirconia are known: monoclinic (M), tetragonal (T), and partially stabilized (e.g., by calcium cations) low-temperature cubic (C) forms [36,37]. We used three zirconia samples: (90% M + 10% T), (60% T + 40% M), and (C + 5% CaO) with particle size varying from 5 to 10 nm. The specific surface of the starting pure support was 74, 150, and 72 m^2/g for the prevalent M, T, and C modifications of zirconia, respectively. Nanosized zirconia (particle size 1.0–1.5 nm), stabilized in the interlayer space (gallery height $\sim$ 0.7 nm) of layered montmorillonite clay (Zr PL) (which differs from bulk ZrO$_2$ in its properties [38]), was used to estimate the size effect of zirconia particles.

The content of the sulfate ions in the catalysts varied from 0.9 to 30 wt.% SO$_4$. The acidic (Lewis and Brønsted) properties of sulfated zirconias were investigated by analyzing the characteristic bands of pyridine in the DRIFT spectra after pyridine adsorption from a methylene chloride solution at room temperature. This method was elaborated in order to be able to compare the acidic properties and activity of the catalysts under similar conditions.

2. Results

2.1. Structural effects of sulfated zirconia

On pure zirconium-containing supports, no transformations of limonene diepoxides **1a,b** have been observed. For sulfated samples, the activity and selectivity with respect to reaction products depend on the modification of zirconia and on the amount of supported sulfate ions. Comparative experiments on the structure effects of sulfated zirconias on the transformations of limonene diepoxides **1a,b** were carried out on samples 1–3 containing 0.9 wt.% SO$_4$ (Table 1). For all these samples, the reaction formed the same products: cyclic alcohol **9** as the major product (Scheme 2 and Table 2) together with minor amounts of tricyclic diethers **6** and **7** (ratio of **9**:**6**:**7** is $\sim$10:1:1, GLC). However, the activity depends on the zirconia polymorphs. Thus after 24 h, conversion of the starting diepoxide was 60% for sample 1, 40% for sample 2, and 100% for sample 3. The highest activity of sample 3 may be attributed to the specific features of sulfate ions on zirconia supports: catalysts based on pseudocubic or monoclinic zirconia are less active than catalysts based on the tetragonal phase. The specific surface area (SSA = 150 m^2/g), as well as the degree of disordering and surface hydroxylation, increased with the proportion of the tetragonal phase (IR and Raman spectral data) [39]. This type of support containing a mixture of the T and M modifications of zirconia was chosen for experiments with varied contents of sulfate ions.

2.2. Effects of the content of sulfate ions

Catalysts containing 0.9–30.3 wt.% SO$_4$ were prepared. Table 1 gives a list of catalyst products. For catalysts prepared by wetness impregnation with an (NH$_4$)$_2$SO$_4$ solution and espe-
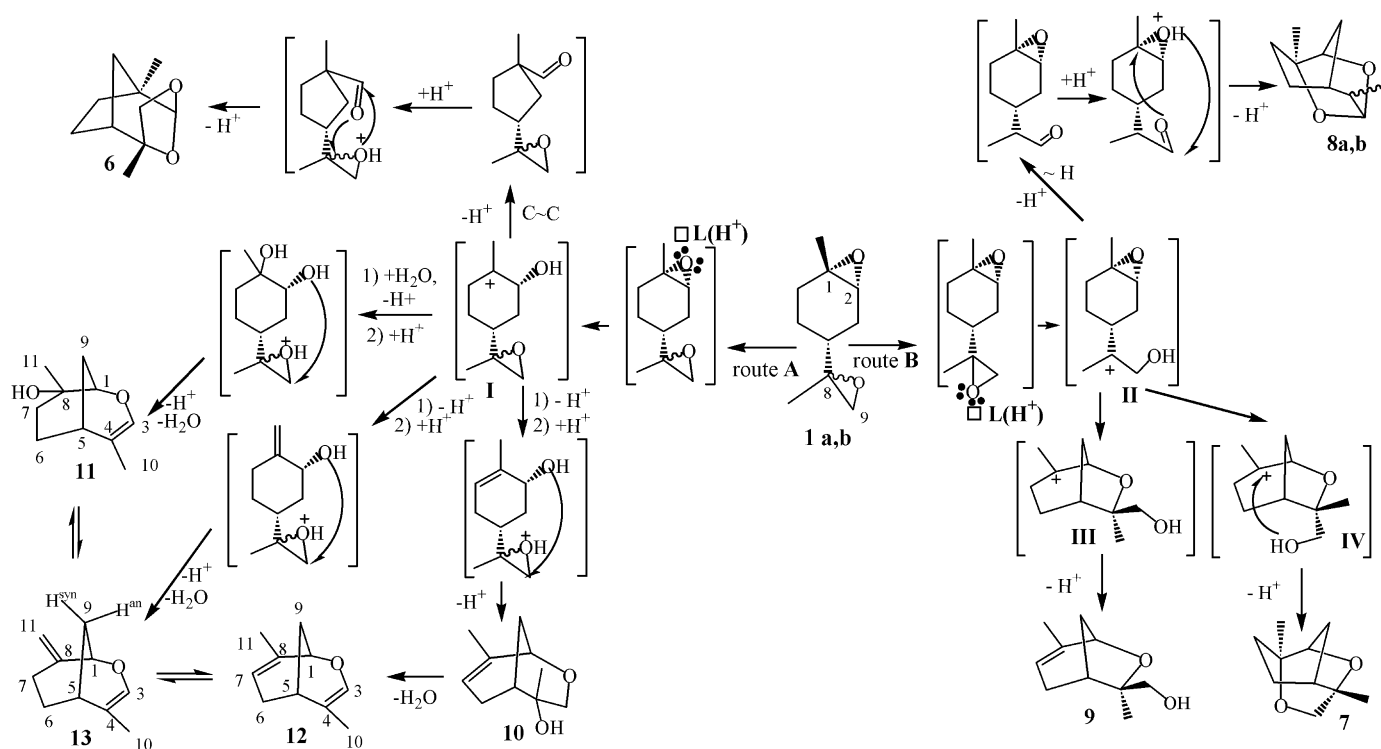
Scheme 2.

cially for catalysts with over 3 wt.% SO$_4$, the specific surface decreased. When sulfate ions are present in high contents, their location along the domain boundaries probably favors the formation of large particles of zirconia, leading to two-dimensional sulfates. Zirconia particles were also observed to enlarge after significant amounts of sulfate ions were added at the stage of synthesis [14].

Table 2 lists data on the transformations of diepoxides **1a,b** on sulfated zirconia with different concentrations of sulfate ions (from 0.9 to 30.3 wt.% SO$_4$). Increased contents of sulfate ions (more than 0.9 wt.% SO$_4$, samples 4–8) led to higher catalyst activity in the transformations of diepoxides **1a,b**; 100% conversion of these compounds was observed even after 5 h (versus 24 h for sample 3) of reaction at room temperature. Isomeriza-

tion of diepoxides **1a,b** on sample 3 containing 0.9 wt.% SO$_4$ selectively formed isobottrospicatol **9** and minor amounts of compounds **6** and **7** (Scheme 2). At higher sulfate concentrations (1.8–3.0 wt.% SO$_4$), the composition of the reaction mixture gradually became more complex: the relative content of compound **9** decreased, while the contents of compounds **6** and **7** increased, and new products appeared in the reaction mixture: **8a,b**, **10**, **11**, **12**, and **13**. For catalysts containing more than 9% sulfate ions, compound **9** was present in minor quantities if at all; the ratio of other compounds did not change significantly. The total peak areas of the products are independent of the composition of the zirconia-based catalysts (Table 2), indicating that the catalysts generally have the same level of activity irrespective of the sulfate ion content. The contribution of other

Table 2
Product ratios in transformations of limonene diepoxides **1a,b** on sulfated catalysts

Catalyst[a]	Product ratio[b]							$\sum$[c]	Selectivity[d] (%)	
	6	**7**	**8a,b**	**9**	**10**	**11**	**12, 13**		Route A	Route B
Sample 3[e]	1.1	1.1	–	10.4	–	–	–	12.6	9	91
Sample 4	1.6	2.5	0.7	8.7	–	–	0.2	13.7	13	87
Sample 5	1.7	2.5	1.9	4.3	1.7	0.6	1.3	14.0	38	62
Sample 6	1.7	2.5	2.0	0.4	3.4	1.1	1.3	12.4	61	39
Sample 7	1.8	2.5	2.1	–	3.7	1.1	1.8	13.0	65	35
Sample 8	1.9	2.4	2.1	–	3.6	1.3	1.8	13.1	66	34
Sample 9	0.4	2.9	–	–	15.5	–	–	18.8	94	6
Sample 10	3.9	3.1	1.0	3.6	2.8	0.9	0.4	15.7	51	49

[a] Reactions conducted in methylene chloride for 5 h, ratio of starting diepoxides **1a:1b** = 3:2, ratio of solid catalyst:diepoxides = 5:2.2 (by mass).
[b] Peak areas given according to GLC data in reaction mixtures with an internal standard whose peak area is taken for unity.
[c] The sum of all peak areas on the chromatogram.
[d] Route A, compounds **6**, **10–13**; route B, compounds **7–9**.
[e] Reaction conducted for 24 h.

types of reactions (e.g., polymerization, oxidation, etc.) did not change with the chemical composition of the catalyst and was up to 10% of the total amount of diepoxides **1a,b** used (evaluated from the weight of the compounds separated from the catalyst). Major differences between the catalysts are reflected by product selectivity and may be caused by varying the structure of active sulfate ions.

Scheme 2 shows the possible mechanism of transformations of diepoxides **1a,b** [6]. The reaction possibly starts with cleavage of the protonated 1,2-epoxy group of diepoxides **1a,b** (route A, compounds **6**, **10–13** as products) or of the protonated 8,9-epoxy group (route B, compounds **7–9** as products). Analysis of the dependence of the product ratio on the catalyst in the transformations of limonene diepoxides **1a,b** (Table 2) revealed that the contribution of reaction route A or B depends on the concentration of the sulfate ions. For catalysts with low contents of sulfate ions, the major reaction products were the compounds that corresponded to the initial cleavage of the 8,9-epoxy group (route B), while increased sulfate ion concentration led to increased contents of products formed by the initial cleavage of the 1,2-epoxy group (route A). Thus activation of polyfunctional terpenoid **1a,b** is rather sensitive to the structure of active centers on the surface.

The relative distribution of isomerization products within groups of compounds formed by different routes also depends on the concentration of the sulfate ions. While compound **6** was present in the reaction mixture in pronounced (but moderate, 8–15%) quantities at any concentration of the sulfate ions, 2-oxabicyclo[3.3.1]nonanes **10–13** formed in significant amounts only on the sample containing 9.0% supported sulfate ions. At higher sulfate concentrations, the relative contents of these compounds in the mixture were practically independent of the catalyst composition.

Compound **9** with a 2-oxabicyclo[3.2.1]octane type framework formed as the major product on samples 3–5, but vanished from the reaction mixture completely when the samples contained more than 9.0% supported sulfate ions. At the same time, tricyclic diether **7** obtained by intramolecular heterocyclization in cation **IV** (Scheme 2) structurally related to cation **III** that forms compound **9** (the only difference being the position – *endo* or *exo* – of the hydroxymethylene group) was present on all sulfated catalysts of the series. Thus varying the concentration of supported sulfate ions is critical not only to the site at which the cation center appears, but also to the stereochemical structure of products.

Reactions of limonene diepoxides **1a,b** with sulfated Zr pillared clay containing 0.9 wt.% SO_4 (sample 10) proceeded more readily than reactions with sample 3 having the same amount of supported sulfate ions. Full conversion of limonene diepoxides **1a,b** on sample 10 was revealed after 5 h of reaction versus 24 h for sample 3. At the same time, transformations of limonene diepoxides **1a,b** over sulfated pillared clay containing smaller zirconia particles (sample 10; 1.0–1.5 nm versus 7.5 nm for 60% T + 40% M) gave a wide range of products with practically equal distributions between routes A and B (Table 2). As a matter of fact, the product ratio is intermediate between the ratios for samples 5 and 6 prepared from bulk zirconia. Pillar clay con-

tains 20 wt.% ZrO_2. When calculated based on bulk zirconia, the content of sulfate ions in this sample is 4.5 %, which is intermediate between the contents of these ions in samples 5 and 6. At the same time, percent of compound **6** in sample 10 is larger, which may be due to the change in the structure of sulfate ions on the surface of nanosized zirconia in pillared clay. Since the latter preferably contains discrete Zr_4 tetramer units, formation of two- and three-dimensional sulfates on deposited sulfate ions was not likely as was the case with bulk ZrO_2 [40]. While pure pillared clay containing nanosized zirconia shows no activity in the transformation of limonene diepoxides **1a,b**, sulfated pillared clay is active in the reaction and gives product distribution other than that in montmorillonite clays. On sample 10, compounds **6**, **7** and **9** formed in approximately equal proportion, while on montmorillonite clay compound **7** was the dominant product [6]. Moreover, transformation of limonene diepoxides **1a,b** on sulfated pillared clay proceeds with formation of new compounds **10–13**. Formation of these compounds may be the result of specific activation of limonene diepoxides **1a,b** on this type of sulfated nanomaterial.

Using alumina instead of zirconia as support for sulfate ions (sample 9) led to substantial changes in the product ratio (Table 2). Compounds formed by route A were the major products. At the same time, on pure alumina no transformations of limonene diepoxides **1a,b** have been detected. The product ratio on sample 9 was similar to that observed previously on the zeolite catalyst [6]. Consequently, the properties of acid centers on the surface of sulfated alumina are similar to the properties of these centers in zeolites, while sulfated zirconia creates other types of acid center. Compounds **10–13** were not detected in the reaction mixture on sample 9 either. These differences may be caused by differences in the structure and properties of sulfates supported to the surface of γ-Al_2O_3 and ZrO_2. While aluminum cations preferably have octahedral surroundings of oxygen atoms, zirconium cations each lies at the center of a cube with coordination number 7 or 8 depending on the structural modification.

Thus the reaction route of limonene diepoxides **1a,b** on the catalysts under study is largely determined by the chemical nature of sulfated active centers.

2.3. Acidity properties

As is known, Lewis and/or Brønsted acidity can easily be determined by using pyridine (Py) adsorption/desorption at RT [41]; IR spectra show well-resolved specific bands that may be attributed either to Lewis acid sites (19b mode of {Py-L} species, $\approx 1445\,cm^{-1}$) or to Brønsted acid sites (19b mode of {Py-B} species, $\approx 1540\,cm^{-1}$). To find out if the differences in the catalytic activity exhibited by different sulfated materials are due to the acidic character of these compounds, we carried out Py adsorption experiments under conditions of limonene diepoxide transformations (details of the method are given below). The difference DRIFT spectra of the samples obtained by subtracting the spectra of {dried methylene chloride + sample} from the spectra of {dried methylene chloride + Py + sample} are shown in Fig. 1. One can clearly see the bands at 1440 and $1540\,cm^{-1}$ ascribed to Lewis and Brønsted acidity centers; the intensity of
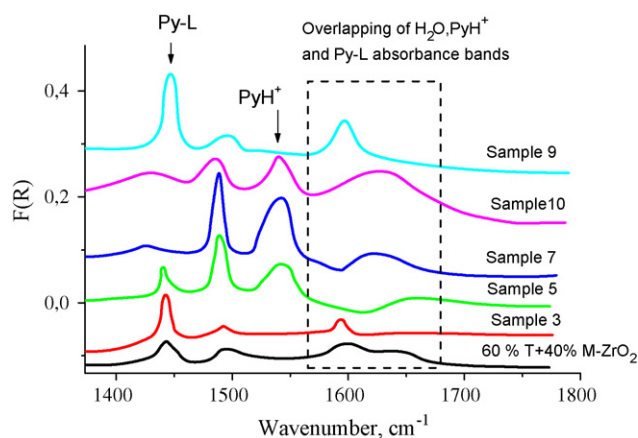
Fig. 1. Difference DRIFT spectra of adsorbed pyridine at RT on the initial support of 60% T + 40% M-ZrO$_2$ and sulfated catalysts (see note in Table 1).

these bands depends on the chemical composition of the catalyst (Table 1). The intensities of other bands, attributed to the overlap of H$_2$O, PyH$^+$, and Py-L absorption bands, are not discussed here. It may be assumed that the observed bands of the {Py-B} and {Py-L} species belong to the rather strong acidic forms on the surface of the catalyst. For the initial support containing 60% T + 40% M-ZrO$_2$, only {Py-L} complexes were observed (Fig. 1), which appeared due to the presence of the surface Zr^{4+} cations with an uncrowded coordination sphere. In spite of the high degree of hydroxylation [39], {Py-B} complexes with surface OH groups did not form on this type of support because of their neutral or basic nature. With small additions of sulfate ions, new Lewis centers can appear due to the interaction with Zr^{4+} cations having an uncrowded coordination sphere. Isolated sulfate ions may change the space near the Zr^{4+} cations, producing complex active centers involving surface hydroxyls. When the addition of sulfate ions increases, the amounts of the {Py-L} species reach a maximum at 0.9 wt.% SO$_4$, while the {Py-B} complexes become visible in the DRIFT spectra at 3 wt.% SO$_4$, increasing at higher sulfate concentrations. The dependence of the number of acidic centers referred to the SSA on the amount of the supported sulfate ions is shown in Fig. 2a. The observed dependences could be explained by the following processes. When sulfate ion additions are small (0.9% SO$_4$), the ions can form new types of Lewis center with Zr^{4+} cations having an uncrowded coordination sphere. The content of this type of defect on the surface of zirconia does not exceed a few percent of the monolayer cover. In this case, Lewis centers can appear due to adsorption on the Zr^{4+} cations having an uncrowded coordination sphere or in the vicinity of these cations, producing complex active centers. At this level of supported sulfate ions, they occupy $\approx$1.5% of the surface area of the support, the occupation area $S_{SO_4} \approx 0.31$ nm^2 included [11]; the SSA of sample 3 practically remains unchanged compared to the area of the initial support. The amount of 3 % SO$_4$ might increase the number of Lewis centers as the sulfate ions occupy only $\approx$3% of the total area. In reality, however, Lewis centers decrease in number, and Brønsted centers appear. The SSA of sample 5 also decreases relative to that of the initial support. At higher contents of sulfate ions, only Brønsted centers
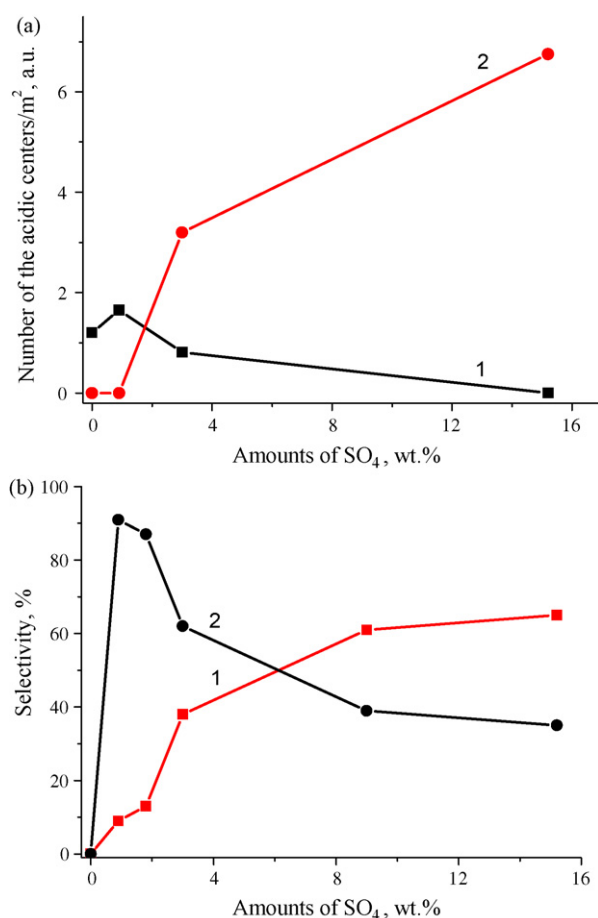

Fig. 2. Numbers of surface Lewis (1) and Brønsted (2) acidic centers per m^2 (a) and selectivity of transformations of limonene diepoxides **1a,b**, route A (1) and route B (2) (b) vs. the amounts of sulfate groups on the surface of ZrO$_2$.

are detected, the SSA diminishing noticeably. Thus an "island" model of sulfate centers may be proposed based on these data. After addition of sulfate ions, Brønsted centers appear around Lewis type centers, probably forming along the microdomain boundary and leading to sintering.

For Zr PL containing nanosized particles of ZrO$_2$ smaller than those of bulk zirconias studied here, sulfation leads to only Brønsted centers detected by Py adsorption (Fig. 1). As a matter of fact, pure Zr PL is characterized by high density of Lewis type Zr^{4+} cations having an uncrowded coordination sphere and detected by CO adsorption; it also has high density of surface hydroxyls originating from Zr$_4$ tetramers [38], while the acidic sites of initial montmorillonite are suppressed by intercalation of the tetramers. According to analysis of low-temperature adsorption of nitrogen [42], the interlayer space in pillared clay is filled with isolated Zr$_4$ tetramers and sheetlike Zr$_8$ species separated by ~0.7–1.0 nm and bound with montmorillonite layers. After sulfation, isolated sulfate species that are Lewis and/or Brønsted centers by nature could appear. Due to the high density of the surface hydroxyls, Lewis centers are accessible for CO (but not Py) adsorption.

After adsorption of Py by sulfated alumina, only Lewis centers are detected (Fig. 1). It is well known that Py does not form Brønsted complexes with hydroxyls of alumina. After 3 wt.%

SO_4 had been applied to alumina, the SSA of the catalyst did not change as was the case with sulfated zirconia (Table 1, sample 9), which could be evidence of the formation of isolated sulfated species. In fact, it is also well known that the number of centers with an uncrowded coordination sphere on alumina is higher than that on zirconia.

3. Discussion

Thus the transformations of limonene diepoxides were gradually changed by varying the properties of sulfated zirconia-based catalysts. It has been shown for the first time that the mechanism of diepoxide transformations may be changed by varying the concentration and type of acid centers in nanosized SO_4/ZrO_2 (Fig. 2). At a low level of 0.9–3% of sulfation, Lewis centers preferably formed, which are responsible for the initial cleavage of the 8,9-epoxy group of limonene diepoxides (route B). With higher amounts of supported sulfate groups, Brønsted centers are the major species on the surface, giving a variety of products of initial cleavage of both 8,9- (route B) and 1,2-epoxy groups (route A). The type of support affects the structural features of the sulfate ions responsible for activation of limonene diepoxides by route A or B. Activation of limonene diepoxides on Lewis centers formed on sulfated alumina follows route A.

The concentration and type of acid centers also affect the stereochemical composition of the product mixture. In the presence of Lewis centers on zirconia, the compound that formed via cation **III** with an *exo* position of the hydroxymethyl group was the major product. After Brønsted centers appeared along with Lewis centers (for amounts of up to 5 wt.% SO_4), this compound vanished from the reaction mixture; however, the content of the compound formed via intermediate cation **IV** with an *endo* position of the hydromethyl group remained almost constant. Evidently, the environment of the acid center along with its type favors a certain conformation of the reactant molecule.

It has been shown that catalyst activity in transformations of limonene diepoxides depends on the structural modification of sulfated zirconia (T, M or C). For sulfated catalysts, activity changes in the series T > M > C. Optimum disordering and hydroxylation of the T phase surface provides the highest activity of the sulfated catalysts. The lower activity of the sulfated monoclinic versus tetragonal zirconia is thought to be caused by the low symmetry of the strained monoclinic modification as revealed by IR and DR-UV spectra [39], but not by the presence of the trigonal oxide ions in the structure of monoclinic zirconia [43].

4. Experiment

4.1. General

Substrate purity and product composition were analyzed by GLC using a Biochrome-1 chromatograph with a quartz capillary column 13,000 mm × 0.22 mm, SE-54 phase. Flame ionization detector, helium as carrier gas. The reaction products were separated by SiO_2 column chromatography (CzFSR, 100–160 μm). Specific rotation was measured on a Polamat A polarimeter. The element composition of the products was determined from high-resolution mass spectra recorded on a Finnigan MAT 8200 instrument. ^1H and ^{13}C NMR spectra were measured on an AM-400 Bruker spectrometer (operating frequency 400.13 MHz for ^1H and 100.61 MHz for ^{13}C) for $CDCl_3$ or (1:1) CCl_4–$CDCl_3$ solutions of the substances. The signal of chloroform was used as an internal standard (δ_H 7.24 ppm, δ_C 76.90 ppm). The structure of the compounds was determined by NMR from proton spin–spin coupling constants in ^1H–^1H double resonance spectra, and by analyzing ^{13}C NMR spectra using proton selective and off-resonance saturation spectra, 2D ^{13}C–^1H correlated spectroscopy on direct C–H constants (COSY, $^1J_{C,H}$ 135 Hz), and 1D ^{13}C–^1H long-range J modulation difference (LRJMD, $J_{C,H}$ 10 Hz).

4.2. Sample preparation

Zirconias with a prevalent monoclinic or tetragonal modification were prepared from a 0.5 M solution of $ZrOCl_2 \times 8H_2O$ by precipitation with aqueous ammonia at pH 10 with further aging of the deposit. To prepare the dominant monoclinic (M) modification, the deposit was aged by ultraviolet radiation (high-pressure mercury lamp) for 12 h at room temperature. After the deposit was washed with distilled water and then dried and calcined at 500 °C for 4 h, it contained 90% M and 10% T (SSA = 74 m²/g) (XRD data). After the deposit was aged at 100 °C for 53 h, washed with water, dried, and calcined at 500 °C for 4 h, the sample contained 60% T and 40% M (SSA = 150 m²/g) (XRD data). The partially stabilized (5 mol% CaO and 95 mol% ZrO_2) low-temperature cubic modification was prepared by the procedure of [18] using polymerized organometal precursors from calcium nitrate and $ZrOCl_2 \times 8H_2O$; the final calcination temperature of the sample was 500 °C after 6 h (SSA = 72 m²/g).

For pillared clay containing 20 mass% ZrO_2 (SSA = 250 m²/g), details of synthesis are given in ref. [19]. Natural montmorillonite clay was employed for synthesis. The particle size of zirconia (1.0–1.5 nm) was estimated [19] by assuming that two or three Zr_4 tetramers entered the interlayer space of pillared clay.

Zirconium-containing samples and reactive γ-Al_2O_3 (SSA = 185 m²/g) were sulfated by incipient wetness impregnation from a water solution of ammonium sulfate. The final calcination temperature of the samples was 500 °C after 1 h.

The specific surface area of BET (SSA, m²/g) was determined from Ar thermal desorption data.

4.3. Sample characterization

X-ray phase analysis of the samples was carried out using an HZG-4C diffractometer (Cu Kα radiation, flat monochromator) in the 2θ range 1–70°. Zirconia phases were identified by using X-ray data files (PCDF): No. 37-1484 for the monoclinic phase, No. 42-1164 for the tetragonal phase, and No. 27-0997 for the low-temperature pseudocubic phase. The concentration of the monoclinic phase mixed with the tetragonal modification was

determined in the following way:

$$C_{mon} = \frac{I_{1\,1\,1}^{mon} + I_{1\,1\,1}^{-mon}}{I_{1\,1\,1}^{mon} + I_{1\,1\,1}^{-mon} + I_{1\,1\,1}^{tetr}}$$

The crystallite size was determined by the Scherrer equation along the 1 1 1 line for the monoclinic modification, along the 1 0 1 line for the tetragonal form, and along the 2 2 0 line for the cubic form: 10, 7.5, and 5.0 nm, respectively. Nanodisperse zirconia in pillared clay was X-ray amorphous.

Diffuse reflectance infrared Fourier transform spectroscopy (DRIFT) spectra of finely ground samples loaded in a small cell (volume ≈ 0.2 ml) and placed in a chamber of DRS-8000 were recorded at room temperature in air at $2\,cm^{-1}$ resolution in the range 400–$4000\,cm^{-1}$ on a Shumadzu-8300 spectrometer. Dried methylene chloride was added to the sample after standard treatment at $400\,°C$ for 30 min; then the "wet" sample was placed in a special cell of the spectrometer and the DRIFT spectrum was recorded. A solution of Py in dried methylene chloride (0.12 mol/l), which ensures excess of Py over surface centers, was added to the "fresh" portion of the sample, and a DRIFT spectrum was recorded for the "wet" sample in the cell after 5 and 10 min of adsorption. The difference spectra, obtained by subtracting the spectra of dried methylene chloride + sample from the spectra of dried methylene chloride + Py + sample, were used for analyzing the acid centers of the catalysts. It has been shown that the Py adsorption time does not influence the peak area of the complexes. The total peak areas of the 1440 and $1540\,cm^{-1}$ bands were used for estimating the relative amounts of Lewis and Brønsted acid centers, respectively, in arbitrary units (Table 1).

4.4. Transformations of diepoxides 1a,b

Limonene diepoxides obtained from R-(+)-limonene (Aldrich, purity 97%, optical purity 98%) by the procedure of [44] were employed; isomer ratio **1a**:**1b** = 3:2 ($[\alpha]_{580}^{20} + 35.5$ (c 3.5, CHCl$_3$)) before the reaction the catalysts were calcinated at $400\,°C$ for 30 min. Dried methylene chloride (2 ml) was added to the solid catalyst (0.05 g). Limonene diepoxides **1a,b** (0.022 g) were added with stirring to the resulting suspension. The mixture was stirred for 5 h and then filtered through an alumina layer (second degree of activity). Then a solution of the internal standard (0.3 ml) was added to the reaction mixture. The resulting reaction mixture was analyzed by GLC. A hexane solution of dicyclopentadiene (10 mg of dicyclopentadiene dissolved in 10 ml of hexane) was used as an internal standard for chromatography. The analytical data are given in Table 2.

Compounds **11**–**13** did not form on any of the previously used catalysts [4–6]; compounds **11** and **13** are not described in the literature. For structure elucidation of compounds **11**–**13** we performed transformation of limonene diepoxides with larger amounts of the initial product. Dried methylene chloride (20 ml) was added to sample 7 (2.00 g). Limonene diepoxides (1.50 g) were added with stirring to the resulting suspension. After 5 h, the reaction mixture was filtered off from the solid catalyst through an alumina layer (second degree of activity, diethyl ether as eluent). The mass of the reaction mixture was 1.40 g. A series

of chromatographic separations on a SiO$_2$ column (hexane with a gradient of diethyl ether from 0 to 80% as eluent) gave a mixture of compounds **12** and **13** (0.025 g, yield 2%), **6** (0.05 g, 3%), **8a,b** (0.03 g, 2%), **3** (0.07 g, 5%), **11** (0.01 g, 1%), and **10** (0.21 g, 14%). A sequence of separations on silica gave compound **11** and a mixture of compounds **12** and **13**. The low total yield of the products is explained by the difficulties of separating structurally related compounds.

(1R,5R)-4,8-Dimethyl-2-oxabicyclo[3.3.1]non-3-en-8-ol (**11**). $[\alpha]_{580}^{20} + 54.5$ (c 1.1, CHCl$_3$). MS, m/z: 168.12338 [M$^+$] C$_{10}$H$_{17}$O$_2$. ^{1}H NMR, δ: 1.24 (s, C^{11}H$_3$), 1.37 (d.d.d.d, H^{7e}, $J_{7e,7a}$ 13 Hz, $J_{7e,6a}$ 4 Hz, $J_{7e,6e}$ 2 Hz, $J_{7e,1}$ 1.5 Hz), 1.48 (d.d.d.d.d, H^{6e}, $J_{6e,6a}$ 13 Hz, $J_{6e,7a}$ 5 Hz, $J_{6e,7e}$ 2 Hz, $J_{6e,5}$ 2 Hz, $J_{6e,9an}$ 2 Hz), 1.51 (d, C^{10}H$_3$, $J_{10,3}$ 1.5 Hz), 1.58 (d.d.d, H^{7a}, J 13 Hz, $J_{7a,6a}$ 13 Hz, $J_{7a,6e}$ 5 Hz), 1.59 (d.d.d.d, H^{9an}, J 13 Hz, $J_{9an,1}$ 4 Hz, $J_{9an,5}$ 4 Hz, $J_{9an,6e}$ 2 Hz), 1.72 (d.d.d.d, H^{6a}, J 13 Hz, $J_{6a,7a}$ 13 Hz, $J_{6a,7e}$ 4 Hz, $J_{6a,5}$ 3.5 Hz), 2.03 (m, H^5), 2.14 (d.d.d, H^{9syn}, J 13 Hz, $J_{9syn,5}$ 2.5 Hz, $J_{9syn,1}$ 1.5 Hz), 3.72 (d.d.d.d, H^1, $J_{1,9an}$ 4 Hz, $J_{1,5}$ 1.5 Hz, $J_{1,7e}$ 1.5 Hz, $J_{1,9syn}$ 1.5 Hz) 6.15 (q, H^3, $J_{3,10}$ 1.5 Hz). ^{13}C NMR, δ: 75.76 (d, C^1), 137.40 (d, C^3), 109.53 (s, C^4), 30.01 (d, C^5), 24.93 (t, C^6), 31.89 (t, C^7), 72.53 (s, C^8), 25.38 (t, C^9), 16.94 (q, C^{10}), 28.34 (q, C^{11}).

Compounds **12** and **13** were not isolated as individual compounds. NMR spectra were recorded for the $\sim$1:0.2 mixture of compounds **12** and **13**: (1R,5R)-4,8-dimethyl-2-oxabicyclo[3.3.1]non-3,7-dien (**12**). ^{1}H NMR, δ: 1.54 (d, C^{10}H$_3$, $J_{10,3}$ 1.5), 1.61 (d.d.d, H^{9syn}, $J_{9syn,9an}$ 12.5, $J_{9syn,1}$ 2.5, $J_{9syn,5}$ 2), 1.75 (d.d.d, C^{11}H$_3$, $J_{11,6'}$ 2.5, $J_{11,6}$ 1.5, $J_{11,7}$ 1.5), 1.85 (d.d.d.d, H^{9an}, J 12.5, $J_{9an,5}$ 4, $J_{9an,1}$ 3, $J_{9an,6}$ 1.5), 2.07 (d.d.d.d.d, H^6, $J_{6,6'}$ 17, $J_{6,7}$ 5, $J_{6,11}$ 1.5, $J_{6,5}$ 1.5, $J_{6,9an}$ 1.5), 2.11 (m, H^5), 2.18 (d.m, H$^{6'}$, J 17), 4.26 (br.d.d, H^1, $J_{1,9ah}$ 3, $J_{1,9syn}$ 2.5), 5.55 (d.d.q, H^7, $J_{7,6}$ 5, $J_{7,6'}$ 2, $J_{7,11}$ 1.5), 6.06 (q, H^3, $J_{3,10}$ 1.5). ^{13}C NMR, δ, м.д: 70.05 (d, C^1), 135.22 (d, C^3), 109.95 (s, C^4), 28.77 (d, C^5), 31.26 (t, C^6), 123.96 (d, C^7), 131.76 (s, C^8), 28.06 (t, C^9), 17.21 (q, C^{10}), 21.44 (q, C^{11}). (1R,5R)-4-Methyl-8-methylen-2-oxabicyclo[3.3.1]non-3-en (**13**). The ^{1}H NMR spectrum contained the following signals (δ): 1.55 (d, C^{10}H$_3$, $J_{10,3}$ 1.5), 1.69 (d.d.d, H^{9syn}, $J_{9syn,9an}$ 12.5, $J_{9syn,5}$ 2.5, $J_{9syn,1}$ 2), 1.94 (d.d.d.d, H^{9an}, J 12.5, $J_{9an,1}$ 4, $J_{9an,6}$ 3.5, $J_{9an,5}$ 2.5), 2.36 (d.d.d.d.d, H^{7a}, $J_{7a,7e}$ 14.5, $J_{7a,6a}$ 13, $J_{7a,6e}$ 6, $J_{7a,11}$ 2, $J_{7a,11'}$ 2), 4.48 (m, H^1), 4.71 (d.d, H^{11}, $J_{11,7a}$ 2, J 2), 4.77 (d.d, H$^{11'}$, $J_{11',7a}$ 2, J 2), 6.32 (q, H^3, $J_{3,10}$ 1.5). The centers of the following proton multiplets were determined from the 2D ^{13}C–^{1}H correlated spectrum on direct constants: 2.13 (m, H^5), 1.54 m and 1.78 m (2H^6), 2.16 (m, H^{7e}). ^{13}C NMR, δ: 74.74 (d, C^1), 138.36 (d, C^3), 109.41 (s, C^4), 30.44 (d, C^5), 30.00 (t, C^6), 27.69 (t, C^7), 149.23 (s, C^8), 31.23 (t, C^9), 16.95 (q, C^{10}), 111.33 (t, C^{11}).

References

[1] J.G. Smith, Synthesis (1984) 629.
[2] V.G. Drjuk, V.G. Kartsev, M.A. Vojtsehovskaja, Oxiranes—Synthesis and Biological Activity, Bogorodsky Pechatnik, Moscow, 1999, p. 528 (Rus.).
[3] N.F. Salakhutdinov, V.A. Barkhash, Usp. Khim. 66 (1997) 376;
N.F. Salakhutdinov, V.A. Barkhash, Russ. Chem. Rev. 66 (1997) 343.

[4] L.A. Mukhamedova, F.G. Nasybullina, M.I. Kudryavtseva, Izv. Akad. Nauk. SSSR, Ser. Khim. 28 (1979) 847.

[5] O.V. Salomatina, O.I. Yarovaya, D.V. Korchagina, Y.u.V. Gatilov, M.P. Polovinka, V.A. Barkhash, Zh. Org. Khim. 42 (2006) 1333;
O.V. Salomatina, O.I. Yarovaya, D.V. Korchagina, Y.u.V. Gatilov, M.P. Polovinka, V.A. Barkhash, Russ. J. Org. Chem. 42 (2006) 1313.

[6] O.V. Salomatina, O.I. Yarovaya, D.V. Korchagina, M.P. Polovinka, V.A. Barkhash, Mendeleev Commun. (2005) 59.

[7] Y. Noma, H. Nishimura, Agric. Biol. Chem. 51 (1987) 1845.

[8] G.T. Maatooq, A.A. Gohar, J.J. Hoffmann, Pharmazie 57 (2002) 282.

[9] S. Hatakeyama, M. Kawamura, E. Shimanuki, S. Takano, Tetrahedron Lett. 33 (1992) 333.

[10] M. Hino, S. Kobayashi, K. Arata, J. Am. Chem. Soc. 101 (1979) 6439.

[11] N. Katada, J. Endo, K. Notsu, N. Yasunobu, N. Naito, M. Niwa, J. Phys. Chem. 104 (2000) 10321.

[12] C. Morterra, G. Cerrato, G. Meligrana, M. Signoretto, F. Pina, G. Strukul, Catal. Lett. 73 (2001) 113.

[13] C.B. Chaabene, L. Bergaoui, A. Ghorbel, J.F. Lambert, P. Grange, Appl. Catal. A 252 (2003) 411.

[14] M.G. Cutrufello, U. Diebold, R.D. Gonzalez, Catal. Lett. 101 (2005) 5.

[15] A. Corma, A. Martinez, C. Martinez, J. Catal. 149 (1994) 52.

[16] D.L. Negelein, R. Lin, R.L. White, J. Appl. Polym. Sci. 67 (1998) 341.

[17] M. Nino, K. Arata, Chem. Lett. (1981) 1671.

[18] G.K. Chuah, S.H. Liu, S. Jaenicke, L.J. Harrison, J. Catal. 200 (2001) 352.

[19] S. Ardizzone, C.L. Bianchi, G. Cappelletti, J. Porta, J. Catal. 227 (2004) 470.

[20] R.S. Drago, N. Kob, J. Phys. Chem. B 101 (1997) 3360.

[21] V. Adeeva, H.-Y. Liu, B.-Q. Xu, W.M.H. Sachtler, Top. Catal. 6 (1998) 61.

[22] D. Fărcaşiu, J.Q. Li, A. Kogelbauer, J. Mol. Catal. 124 (1997) 67.

[23] T.-K. Cheung, B.C. Gates, Top. Catal. 6 (1998) 41.

[24] C. Morterra, G. Cerrato, S. Ardizzone, C.L. Bianchi, M. Signoretto, F. Pina, Phys. Chem. Chem. Phys. 4 (2002) 3136.

[25] M. Waquif, J. Bachelier, O. saur, J.-C. lavalley, J. Mol. Catal. 72 (1992) 127.

[26] T. Yamaguchi, Appl. Catal. 61 (1990) 1.

[27] A. Clearfield, G.P.D. Serrette, A.H. Khazi-Syed, Catal. Today 20 (1994) 295.

[28] M. Benaissa, J.D. Santiesteban, G. Diaz, C.D. Chang, M. Jose-Yacaman, J. Catal. 161 (1996) 694.

[29] C.R. Vera, J.M. Parera, J. Catal. 165 (1997) 254.

[30] A.F. Bedilo, K.J. Klabunde, J. Catal. 176 (1998) 448.

[31] V. Parvulescu, S. Coman, P. Grange, V.I. Parvulescu, Appl. Catal. A 176 (1999) 27.

[32] S.X. Song, R.A. Kydd, J. Chem. Soc., Faraday Trans. 94 (1998) 1333.

[33] F. Babou, B. Bigot, P. Sautet, J. Phys. Chem. 97 (1993) 11501.

[34] F. Haase, J. Sauer, J. Am. Chem. Soc. 120 (1998) 13503.

[35] B. Umansky, J. Engelharrdt, W.K. Hall, J. Catal. 127 (1991) 128.

[36] K.T. Jung, A.T. Bell, J. Mol. Catal. A: Chem. 163 (2000) 27.

[37] T.G. Kuznetsova, V.A. Sadykov, E.M. Moroz, S.N. Trukhan, E.A. Paukshtis, V.N. Kolomiichuk, E.B. Burgina, V.I. Zaikovskii, M.A. Fedotov, V.V. Lunin, E. Kemnitz, Stud. Surf. Sci. Catal. 143 (2002) 659.

[38] V.A. Sadykov, T.G. Kuznetsova, V.P. Doronin, et al., Top. Catal. 32 (2005) 29.

[39] T. Kuznetsova, V. Sadykov, L. Batuev, E. Burgina, E. Moroz, et al., Proc. Fourth Asia Pacific Congress on Catalysis, Singapore, 2006.

[40] V. Sadykov, T. Kuznetsova, V. Doronin, et al., Catal. Today 114 (2006) 13.

[41] E.P. Parry, J. Catal. 2 (1963) 371.

[42] D. Efremov, T. Kuznetsova, V. Doronin, V. Sadykov, J. Phys. Chem. B 109 (2005) 7451.

[43] E.F. Lopez, V.S. Escribano, M. Panizza, M.M. Carnasciali, G. Busca, J. Mater. Chem. 11 (2001) 1891.

[44] V.A. Startzeva, L.A. Nikitina, V.V. Plemenkov, Zh. Org. Khim. 37 (2001) 46;
V.A. Startzeva, L.A. Nikitina, V.V. Plemenkov, Russ. J. Org. Chem. 37 (2001) 34.